

Sky monitoring with ARGO-YBJ

S. Vernetto*, Z. Guglielmotto[†], J.L. Zhang[‡], on behalf of the ARGO-YBJ Collaboration

**IFSI-INAf and INFN Torino, Italy*

[†]*Dipartimento di Fisica Generale dell'Università di Torino, Torino, Italy*

[‡]*Institute of High Energy Physics, Chinese Academy of Science, Beijing, P.R. China*

Abstract. A sky monitoring at gamma ray energy $E > 0.6$ TeV has been performed by the full coverage Extensive Air Shower detector ARGO-YBJ, located in Tibet at 4300 m of altitude. We monitored 135 galactic and extragalactic gamma ray sources in the sky declination band from -10° to $+70^\circ$ for 424 days, detecting the Crab Nebula and Mrk421 with a significance respectively of 7.0 and 8.0 standard deviations. For a set of 11 AGNs known to emit in the TeV energy range, the search has been performed in time scales of 1, 10 and 30 days in order to study possible flaring activities. Significant emissions has been observed from Mrk421 in the time scales of 10 and 30 days, during June and March 2008, when the source had a strong activity also observed in the X-rays waveband.

The analysis of the background has revealed the existence of a significant excess of the CR flux in two localized regions of angular size 10° – 30° , in agreement with previous indications.

Keywords: gamma ray sources, AGN, air showers

I. THE DETECTOR

ARGO-YBJ is a full coverage air shower detector located at the Yangbajing Cosmic Ray Laboratory (Tibet, P.R. China, lat 30.1N, long 90.5E, 4300 m a.s.l.). Due to its large field of view (~ 2 sr) and its high duty cycle ($>90\%$) it can monitor continuously a large fraction of the sky, searching for gamma rays sources at energy $E > 0.6$ TeV.

The apparatus is composed of a central carpet of Resistive Plate Chambers (RPCs) ($\sim 74 \times 78$ m², $\sim 93\%$ of active area) enclosed by a guard ring with partial coverage, which allows to extend the instrumented area up to $\sim 100 \times 110$ m². The basic data acquisition element is a cluster (5.7×7.6 m²), made of 12 RPCs (2.8×1.25 m²). Each chamber is read by 80 strips of 6.75×61.8 cm² (the spatial pixel), logically organized in 10 independent pads of 55.6×61.8 cm² which are individually acquired and represent the time pixel of the detector. The full detector is composed of 153 clusters for a total active surface of ~ 6600 m² [1].

Operated in *shower mode* ARGO-YBJ records all events with a number of fired pads $N_{pad} \geq 20$ in the central carpet, detected in a time window of 420 ns. The spatial coordinates and the time of any fired pad are then used to reconstruct the position of the shower core and the arrival direction of the primary[2].

The installation of the detector has been completed in autumn 2007 and since November 2007 ARGO-YBJ is in stable data taking with a trigger rate of ~ 3.6 KHz.

The angular resolution and the pointing accuracy of the detector have been evaluated by using the Moon shadow, i.e. the deficit of cosmic rays in the Moon direction.[3]. According to the Moon shadow data, the PSF of the detector is Gaussian for $N_{pad} \geq 100$, while for lower multiplicities it can be described with an additional Gaussian, which contributes for about 20%. The obtained values of the radius ψ containing $\sim 71.5\%$ of the signal, are $2.59^\circ \pm 0.16^\circ$, $1.30^\circ \pm 0.14$ and $1.04^\circ \pm 0.12^\circ$ respectively for $N_{pad} \geq 40, 100$ and 300 , in agreement with expectations from Monte Carlo simulations. This measured angular resolution refers to cosmic rays-induced air showers. The angular resolution for γ -induced events has been evaluated by simulations and it is 10-30% smaller (depending on N_{pad}), due to the better defined time profile of the showers.

II. SKY MONITORING

The data used in this analysis have been recorded from 2007 day 311 to 2009 day 89 for a total live time of 424 days. All events with a zenith angle $\theta < 40^\circ$ and a number of hit pads on the central carpet $N_{pad} \geq 40$ have been considered. The events with a large value of the χ^2 resulting from the fitting procedure for the arrival direction determination, have been discarded from the analysis.

With these events, five sky maps in celestial coordinates are built, for different number of hit pads: $N_{pad} \geq 40, 60, 100, 200, 300$. The maps are produced with the HEALPix package (Hierarchical Equal Area isoLatitude Pixelization)[4]. Each map has $\sim 3.14 \cdot 10^6$ pixels of equal area ~ 0.013 squared degrees. The observed sky covers the declination band from -10° to 70° .

The background is evaluated with the *time swapping* method [5]. For each detected event, 10 "fake" events are generated by replacing the original arrival time with new ones, randomly selected from a buffer that spans about 4 hours of data taking. For every N_{pad} interval, the "event" map and the "background map" are then integrated over a circular area of radius ψ , i.e. every bin is filled with the content of all bins whose center has an angular distance less than ψ from its center. The value of the smoothing radius, related to the angular resolution, is the angle that maximizes the signal to noise ratio from a Crab-like source, according to simulations, i.e. $\psi = 1.3^\circ$,

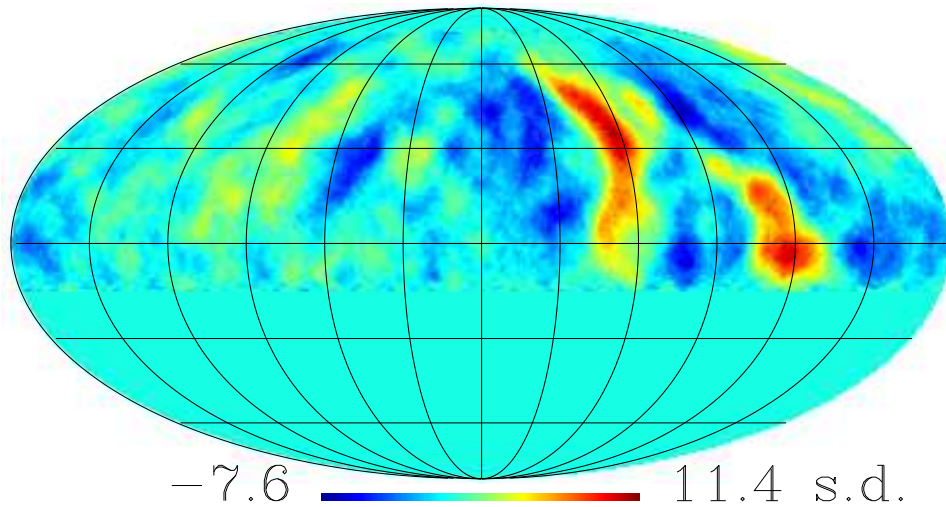


Fig. 1: Sky map in equatorial coordinates obtained in 424 days of measurements, for events with $N_{pad} \geq 40$. The right ascension is equal to zero on the extreme right of the map and increases going towards the left. The color scale indicates the statistical significance in standard deviations.

0.7° and 0.5° respectively for $N_{pad} \geq 40$, 100 and 300. Finally the background map is subtracted to the relative event map, obtaining the "signal map", where for every bin the statistical significance of the excess is calculated.

Fig 1. shows the sky map for events with $N_{pad} \geq 40$, obtained with a smoothing radius $\psi=5^\circ$, adding the data of the whole period. The map shows two large hot spots in the region of the Galactic anticenter, already reported by the Milagro detector[6]. These regions have been interpreted as excesses of cosmic rays, but the origin is not yet understood. They could be related to the observed large scale anisotropy of cosmic rays due to the propagation of cosmic rays in the galactic magnetic field [7], [8]. Some authors discuss the possibility of the hot spots being due to a galactic nearby source as a supernova explosion in the recent past[9], [10]. The two excesses (> 10 standard deviations, corresponding to a flux increase of $\sim 0.1\%$) are observed by ARGONAT around the positions $\alpha \sim 120^\circ$, $\delta \sim 40^\circ$ and $\alpha \sim 60^\circ$, $\delta \sim -5^\circ$. in agreement with the Milagro detection, even if the maximum of the second excess is slightly shifted towards lower declinations, probably because ARGONAT can observe with more efficiency the southern regions of the sky, being located at a smaller latitude than Milagro. The two hot spots are also present in the map corresponding to events with a larger number of pad, even if with less significance due to the reduced statistics. The median primary energy E_m corresponding to proton showers with $N_{pad} \geq 40$ (300) is ~ 2 (10) TeV.

The deficit regions parallel to the excesses are due to a known effect of the analysis, that uses also the excess events to evaluate the background, artificially increasing the background.

The analysis of these hot spots will be the subject of a

forthcoming paper. In this work, we refer to them only since they affect the point gamma ray source search. In fact the time swapping method applied over a time interval of 4 hours makes the analysis insensitive to features of scale larger than $\sim 60^\circ$, but all excesses of a smaller extension constitute a kind of "noise" for the point source search. If a source is located inside an excess region, its significance will be overestimated, and vice versa.

In order to renormalized the background eliminating all features of size $10-20^\circ$, we multiplied the content of each bin of the background map by a correction factor $f=E/B$, where E and B are respectively the numbers of events of the event map and background map inside a circle of radius 8° centered on that bin, excluding the events from the circle central region up to a radius of 3.5° to avoid that a possible source affects the evaluation of E. Fig. 2 shows the sky map after the correction. The Crab Nebula and Mrk421 are visible with a statistical significance respectively of 7.0 and 8.0 standard deviations. The obtained Crab energy spectrum is in agreement with the observations by other experiments[11]. Mrk421 had many active states during 2008, in particular during March and June, and has been deeply studied by ARGONAT in a dedicate paper[12].

Excluding the bins around the Crab and Mrk421 positions, the distribution of the excesses well fits to a Gauss distribution with mean value $= -3.6 \pm 0.8 \cdot 10^{-3}$ and r.m.s. $= 1.01 \pm 5 \cdot 10^{-4}$ (Fig.3).

As a second step, we analysed the maps contents at the positions of several known gamma rays sources. We adopted two gamma ray source catalogues:

a) the recently published list of bright sources observed by Fermi at $E > 100$ MeV[13]

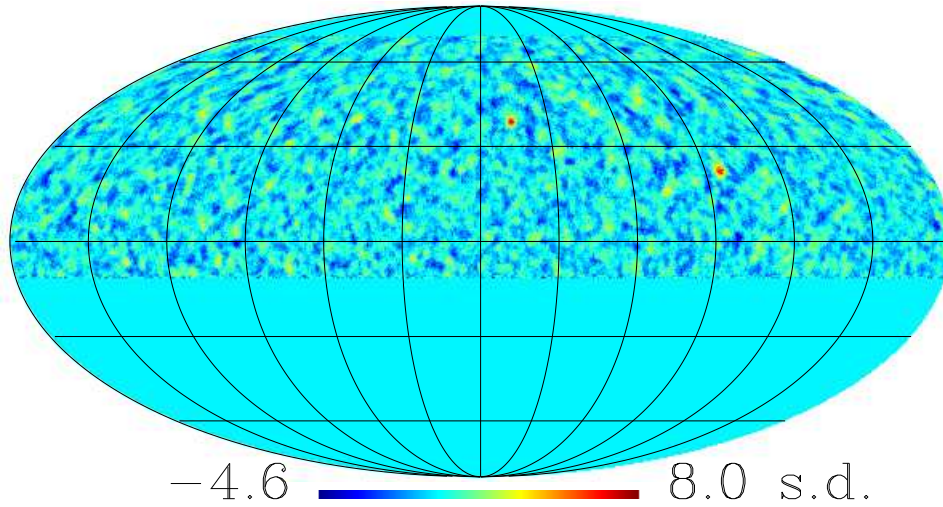


Fig. 2: Sky map after correction, for events with $N_{pad} \geq 40$. The Crab Nebula and Mrk421 are observed with a statistical significance respectively of 7.0 and 8.0 standard deviations.

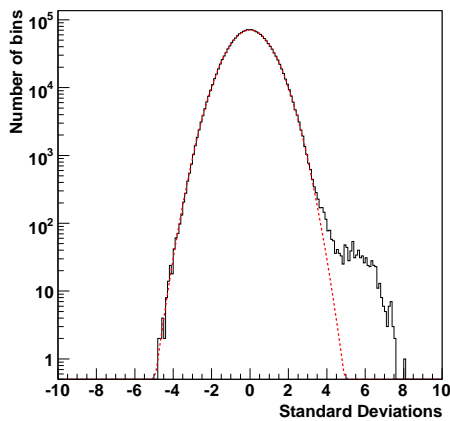


Fig. 3: Distribution of the sky map excesses for events with $N_{pad} \geq 40$. The red dashed line represents the Gaussian fit.

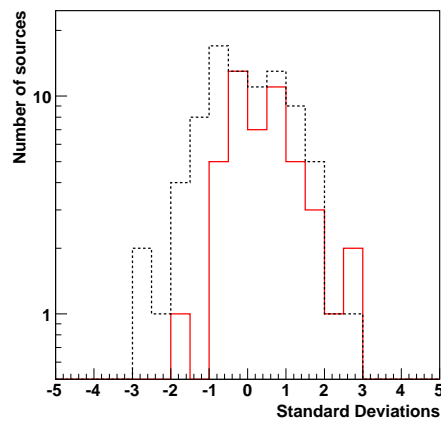


Fig. 4: Distribution of the excesses observed at the position of 133 gamma ray sources (black dashed line: extragalactic sources, red solid line: galactic sources)

b) the list of sources seen at $E > 100$ GeV[14]

containing respectively 115 and 44 sources in the declination band corresponding to the ARGO-YBJ field of view, of which 24 are contained in both lists. Merging the two catalogues, we got a list of 135 sources, 86 extragalactic and 49 galactic (or unidentified but lying close to the galactic plane). For every source the radius r of the observational window is set to ψ , unless the source is known to be extended. In this case $r = \sqrt{(\psi^2 + \alpha^2)}$ where α is equal to half the angular size.

The median energy E_m corresponding to gamma rays showers with a given number of pads depends on the source spectrum and on the culmination zenith angle. For $N_{pad} \geq 40$ the median energy ranges from ~ 0.6 TeV (for a source culminating at the zenith and with

a steep spectrum like E^{-3}) up to ~ 2 TeV (for a source culminating at 20° with a $E^{-2.5}$ spectrum).

Fig. 4 shows the statistical significance of the observed sources, excluding the Crab Nebula and Mrk421, for $N_{pad} \geq 40$. No source shows a significance larger than 4 standard deviations, however the mean value of the distribution of the excesses for galactic sources is clearly shifted towards positive values (0.45 ± 0.14) while the mean value for extragalactic sources is compatible with zero (-0.02 ± 0.12).

We found 2 objects with a significance larger than 3 s.d for $N_{pad} \geq 60$, namely:

a) MGROJ1908+06 with 3.2 s.d. (discovered by Milagro[15], confirmed by Hess[16] and recently associated to the Fermi pulsar 0FGL J1907+5+0602)[17];

TABLE I: AGNs observation: for each source is given a) the redshift, b) the culmination zenith angle θ_c , c) the hours of observation per day, d) the flux above 0.6 TeV.

Source	z	θ_c (deg)	h/day	Flux ($E > 0.6$ TeV) $\text{ph cm}^{-2}\text{s}^{-1}$
M87	0.004	17.7	5.2	$< 3.4 \cdot 10^{-11}$
Mrk421	0.031	8.1	6.4	$5.5 \pm 0.7 \cdot 10^{-11}$
Mrk501	0.034	9.6	6.4	$< 2.7 \cdot 10^{-11}$
BL Lacertae	0.069	12.2	6.4	$< 1.7 \cdot 10^{-11}$
W Comae	0.102	1.9	6.1	$< 2.4 \cdot 10^{-11}$
1H 1426+428	0.129	12.6	6.4	$< 2.6 \cdot 10^{-11}$
1ES 0229+200	0.140	9.8	5.8	$< 2.5 \cdot 10^{-11}$
1ES 1218+304	0.182	0.1	6.2	$< 1.9 \cdot 10^{-11}$
1ES 1011+496	0.212	19.3	6.2	$< 2.9 \cdot 10^{-11}$
PG 1553+113	0.360	18.9	5.1	—————
3C 66A	0.444	12.9	6.4	—————

b) the unidentified HESS source HESSJ1841-055, with 3.0 s.d.;

Considered the number of trials (133 sources \times 5 N_{pad} intervals) and the small significance of the excesses it is difficult to say if they are due to gamma rays or to a background fluctuation. Moreover the corresponding flux is larger than what expected from these source, in particular for HESSJ1841-055[18].

III. AGN FOLLOW UP

Since AGNs are known to be variable on different time scales, we have monitored the time behaviour of a subset of 11 AGNs known to emit at $E > 100$ GeV, and having a culmination zenith angle $< 20^\circ$ in our field of view (see Tab.1).

The sources have been studied on time scales of 1, 10 days and 30 days. For this analysis we have considered the data taken in the period 2007 day 311 - 2009 day 89.

Concerning the daily search, we found only one excess with a significance larger than 4 s.d. (4.3 s.d.), from the blazar 1ES0229+200 on 2008 day 259, for $N_{pad} \geq 40$. However, considering the number of trials (11 sources \times 510 days \times 5 N_{pad} intervals) this excess is consistent with a background fluctuation.

Concerning the 10 days analysis, the only excess larger than 4 s.d. is due to Mrk421 in the time intervals 2008 days 161-170 (4.6 s.d.) during a strong X-ray flare.

Looking for 30 days excess, the search has been done shifting the 30 days interval in steps of 10 days. Also in this case we found several excesses from Mrk421 with significances between 4 and 5 s.d., in particular in the intervals: 2008 days 1-30, 71-100, 81-110, 91-120, 141-170, when several X-Ray flares have been observed[19].

For all sources except Mrk421 (for which we give the observed flux) we calculate the upper limit to the flux at a confidence level of 3 standard deviations. For each source we assumed a power law spectrum with a fixed spectral slope: $dN/dE = K E^{-2.5}$ multiplied by an exponential factor $e^{-\tau(E,z)}$ to take into account the absorption of gamma rays on the Extragalactic Background Light (EBL). We evaluated $\tau(E,z)$ interpolating the

curves given by Primack et al.[20] for fixed redshifts in the range $z=0.03-0.3$. Lacking the absorption parameters outside this range, the upper limit for 3C66A ($z=0.444$) and PG1553+113 ($z=0.36$) have not been evaluated, while for M87 ($z=0.004$) we assumed no absorption.

From the number of observed events (or the upper limit in case of no detection) the corresponding gamma ray flux is determined by a complete simulation process that evaluates the expected number of events from a source with a given spectrum and a given daily path in the sky. Tab.1 shows the observed integral flux above 0.6 TeV for Mrk421 and the upper limits obtained for the 8 AGNs with no detection, averaged over the whole observation period, for events with $N_{pad} \geq 40$.

To know the minimum flux observable by ARGO-YBJ during a flare of a generic duration n days, one can multiply the upper limits given in the table by a factor $\sqrt{(T/n)}$, where $T=424$ is the total number of days considered in this analysis.

IV. CONCLUSIONS

For a period of ~ 15 months ARGO-YBJ monitored the gamma ray sky in the declination band from -10° to $+70^\circ$. The observations of the background have revealed the existence of two regions with size of order $10^\circ-30^\circ$, where the CR flux is enhanced by approximately 0.1 %. The origin of these medium scale anisotropies, previously observed by the Milagro experiment, remains unexplained.

A search for point sources of high energy gamma radiation has resulted in the detection with high significance of the Crab Nebula and Mrk421.

The data acquisition is currently going ahead with stable detection conditions. Studies to improve the detector sensitivity are in progress, both in the direction of increasing the angular resolution[11] and of rejecting the cosmic rays background[21], implementing gamma-hadron separation algorithms.

REFERENCES

- [1] Aielli G. et al., 2006, NIM A562, 92
- [2] Di Sciascio G. et al., 2007, Proc. 30th ICRC, Merida, Mexico (arXiv:0710.1945)
- [3] Di Sciascio G. et al., 2009, Proc. 31th ICRC, Lodz, Poland
- [4] Gorski et al., 2005, ApJ 622, 759 (<http://healpix.jpl.nasa.gov>)
- [5] Alexandreas D.E. et al., 1992, NIM A311, 350
- [6] Abdo A.A. et al., 2008, Phys.Rev.Lett. 101, 221101
- [7] Zhang J.L. et al., 2009, Proc. 31th ICRC, Lodz, Pol
- [8] Amenomori M. et al., 2006, Science 314, 439
- [9] Drury L. & Aharonian F., 2008, Astrop.Phys. 29, 420
- [10] Salvati M. & Sacco B., 2008, Astron. Astroph. 485, 2, 527
- [11] Martello D. et al., 2009, Proc. 31th ICRC, Lodz, Poland
- [12] Vernetto S. et al., 2009, Proc. 31th ICRC, Lodz, Poland
- [13] Abdo A.A. et al., 2009, arXiv:0902.134v1
- [14] TevCat catalogue: <http://tevcat.uchicago.edu>
- [15] Abdo A.A. et al., 2007, ApJ Lett. 664, 91
- [16] Djannati-Atai A. et al., 2007, Proc. 30th ICRC, Merida, Mexico
- [17] Abdo A.A. et al., 2009, arXiv:0904.1018v1
- [18] Aharonian F. et al., 2008, Astron. Astrophys. 477, 353
- [19] RXTE/ASM public data: <http://xte.mit.edu/asmlc/ASM.html>
- [20] Primack J.R., Bullock J.S., & Somerville R.S., 2005, AIP Conf. Proc. 745, 23
- [21] Dattoli M. et al., 2009, Proc. 31th ICRC, Lodz, Poland